PHYSICAL REVIEW D **89,** 026014 (2014)

AdS-sliced flavor branes and adding flavor to the Janus solution

Adam B. Clark,[*] Nathan Crossette,[†] and Andrea Rommal[‡]
Muhlenberg College, Allentown, Pennsylvania 18104, USA

George M. Newman[§]
Washington State University - Vancouver, Vancouver, Washington 98686-9600, USA
(Received 3 October 2013; published 28 January 2014)

We implement D7 flavor branes in anti-de Sitter-sliced coordinates on $AdS_5 \times S^5$ with the ansatz that the brane fluctuates only in the warped (μ) direction in this slicing, which is particularly appropriate for studying the Janus solution. The natural field theory dual in this slicing is $\mathcal{N} = 4$ super-Yang–Mills on two copies of AdS_4. Branes extending from $\mu = \pm\pi/2$ can end at different locations, giving rise to quarks with a piecewise constant mass on each AdS_4 half-space, jumping discontinuously between them. A second class of flavor brane solutions exists in this coordinate system, dubbed "continuous" flavor branes, which extend across the entire range of μ. We propose that the correct dual interpretation of the "disconnected" flavor brane in this ansatz is a quark hypermultiplet with constant mass on one of the AdS_4 half-spaces with totally reflecting boundary conditions at the boundary of AdS_4; whereas the dual interpretation of a continuous flavor brane has totally transparent boundary conditions. Numerical studies indicate that AdS-sliced D7 flavor branes of both classes exhibit spontaneous chiral symmetry breaking, as a nonzero vacuum expectation value persists for solutions of the equation of motion down to zero mass. Continuous flavor branes in this ansatz exhibit many other surprising behaviors: their masses seem to be capped at a modest value near $m = 0.551$ in units of the inverse AdS radius, and there may be a phase transition between continuous branes of different configurations. We also numerically study quark states in Janus. The behavior of the mass and vacuum expectation value is similar in Janus, including the existence of chiral symmetry breaking at zero mass, though qualitative features of the phase diagram change (sometimes significantly) as the Janus parameter c_0 increases.

DOI: 10.1103/PhysRevD.89.026014 PACS numbers: 11.25.Tq

I. INTRODUCTION

Holography and the AdS/CFT correspondence have been exciting fields of study since their discovery in the late 1990s [1–3]. Matter fields can be added to the gravity side by the well-known prescription of adding a small number, N_f, of "flavor" branes [4]. This breaks half the supersymmetries of the gauge theory. The Janus solution of type IIB supergravity is interesting because locally it is very similar to ordinary anti-de Sitter (AdS) space, but the dilaton and 5-form vary in the warped direction in a particular slicing. This situation breaks supersymmetry entirely yet remains stable. The dual gauge theory is most commonly viewed as an "interface" conformal field theory, that is $\mathcal{N} = 4$ super-Yang–Mills theory with a gauge coupling that jumps suddenly at the interface of a domain wall. The jumping coupling is somewhat analogous to filling half the Universe with a dielectric medium with a planar interface. This analogy is imprecise in one very important way: the speed of light does not change when crossing the domain wall, as it would if the interface were truly that between two dielectric media.

We expect systems that break supersymmetry to generically also break chiral symmetry as the formation of a condensate is no longer forbidden. Janus provides a novel mechanism for this to occur, since supersymmetry in the dual gauge theory is broken by the jumping of the coupling constant. Chiral symmetry will be broken by the same unusual mechanism. More surprisingly, regular AdS space with flavor branes set up according to a Janus-like ansatz also appears to break chiral symmetry.

II. REVIEW OF JANUS SOLUTION

A. Coordinate systems

We review a variety of coordinate systems for AdS_{d+1}, defined as a hyperboloid in $R^{2,d}$:

$$X_0^2 + X_{d+1}^2 - X_1^2 - \cdots - X_d^2 = 1. \tag{1}$$

We will always work with unit radius. If necessary, the AdS curvature radius can be restored with dimensional analysis.

[*]aclark@muhlenberg.edu
[†]npc31@cam.ac.uk
[‡]ar244930@muhlenberg.edu
[§]gmnewman@wsuvancouver.edu

1. Global coordinates

Global coordinates cover the entirety of AdS space. They consist of the following parametrization:

$$X_0 = \frac{\cos\tau}{\cos\theta}, \qquad X_{d+1} = \frac{\sin\tau}{\cos\theta},$$
$$X_i = \tan\theta n_i, \qquad i = 1,\ldots,d, \tag{2}$$

where the n_i are unit vectors on R^d. The coordinate τ fills the timelike role, and θ is the warped direction and is bounded $[0,\pi/2]$. The metric in these coordinates is

$$ds^2_{\mathrm{AdS}_{d+1}} = \frac{1}{\cos^2\theta}(-d\tau^2 + d\theta^2 + \sin^2\theta d\Omega^2_{d-1}). \tag{3}$$

2. Poincaré patch coordinates

Poincaré patch coordinates are often the most convenient coordinates, despite the ugly parametrization

$$X_0 = \frac{1}{2}(z + (1+\vec{x}^2 - t^2)), \qquad X_{d+1} = \frac{t}{z},$$
$$X_d = \frac{1}{2}(z - (1-\vec{x}^2 + t^2)), \qquad X_{i=1,\ldots,d-1} = \frac{x_i}{z}. \tag{4}$$

This gives us the metric

$$ds^2_{\mathrm{AdS}_{d+1}} = \frac{1}{z^2}(-dt^2 + d\vec{x}^2 + dz^2). \tag{5}$$

The timelike coordinate is of course t, z is the warped coordinate bounded $[0,\infty]$, and $\vec{x}$ denotes $(x_1,\ldots..x_{d-1})$. Patch coordinates only cover half of the spacetime. If one defines $u = \frac{1}{z}$, Poincaré patch coordinates can be recast so that the metric takes on the form

$$ds^2_{\mathrm{AdS}_{d+1}} = u^2(-dt^2 + d\vec{x}^2) + \frac{1}{u^2}du^2. \tag{6}$$

When it is necessary to distinguish these two coordinate systems, we will refer to the coordinates with u as "braneworld patch coordinates," as this is the metric that shows up most naturally when taking the near horizon limit of the spacetime created by a stack of coincident D-branes. The coordinate u plays the role of a radius or transverse distance from the branes.

A third variation of Poincaré patch coordinates is sometimes useful. Let $r = \log(u)$. Then the metric becomes

$$ds^2_{\mathrm{AdS}_{d+1}} = e^{2r}(-dt^2 + d\vec{x}^2) + dr^2. \tag{7}$$

3. AdS-sliced coordinates

First, parametrize $X_d = \arctan(\mu)$, where μ is an angle in $[-\pi/2,\pi/2]$. For the remaining hyperboloid coordinates, choose any coordinate system for an AdS space of one lower dimension with variable radius given by $\cos\mu$. The metric becomes

$$ds^2_{\mathrm{AdS}_{d+1}} = \frac{1}{\cos^2\mu}(d\mu^2 + ds^2_{\mathrm{AdS}_d}). \tag{8}$$

We point out a useful identity from Ref. [5]. If we take Poincaré patch coordinates on the AdS_4 slices, the full metric is

$$ds^2_{\mathrm{AdS}_5} = \frac{1}{y^2\cos^2\mu}(-dt^2 + d\vec{x}^2 + dy^2 + y^2 d\mu^2), \tag{9}$$

where y is the warped coordinate on the AdS_4 slices and $\vec{x}$ refers to the two nonwarped spatial directions on the AdS_4 slices. This can be related to conventional Poincaré patch coordinates by the following transformation:

$$x = y\sin\mu$$
$$z = y\cos\mu, \tag{10}$$

where x is a nonwarped direction in conventional Poincaré patch coordinates. For braneworld coordinates, this relation becomes

$$u = \frac{1}{y\cos\mu} = e^r. \tag{11}$$

For more details on the coordinate system, see Refs. [5,6]. We will use the term "Janus-sliced coordinates" as an easier to pronounce alternative to "AdS-sliced coordinates."

B. Janus ansatz

The original Janus solution was an ansatz for a dilaton and 5-form running in the warped direction of a deformed AdS, presented in AdS-sliced coordinates. The deformation alters the warp factor away from $1/\cos^2\mu$ and introduces an "angular excess" [5].

When making the Janus ansatz, the warp factor of AdS_5 is promoted from the fixed function $1/\cos^2\mu$ to a more general $f(\mu)$. The dilaton and 5-form are allowed to run in the μ direction as follows:

$$\phi = \phi(\mu) \tag{12}$$

$$F_5 = 2f(\mu)^{5/2}d\mu\wedge\omega_{\mathrm{AdS}_4} + 2\omega_{S^5}, \tag{13}$$

where the ω's denote unit volume forms on their respective subspaces. With this ansatz, the supergravity equations of motion reduce to

$$\phi'(\mu) = \frac{c_0}{f^{3/2}(\mu)} \tag{14}$$

for the dilaton, where c_0 is an integration constant, and

$$(f')^2 = 4f^3 - 4f^2 + \frac{c_0^2}{6f} \tag{15}$$

for the warp factor. For more detail, see Refs. [5,6]. Equation (15) can be integrated to find the maximum value of μ, dubbed μ_0 [5], and the integral can in turn be evaluated in a series expansion for sufficiently small c_0 [6,7]:

$$\mu_0 = \frac{\sqrt{\pi}}{2}\sum_{n=0}^{\infty}\frac{\Gamma(4n+\frac{1}{2})}{\Gamma(3n+1)n!}\left(\frac{c_0^2}{24}\right)^n. \tag{16}$$

It is worth noting that Eq. (15) has four zeros in f, but only two of them are real and only for the choice $0 \le c_0 \le \frac{9}{4\sqrt{2}} \approx 1.59$. So to find a physical solution, one must choose the integration constant c_0 within that range and choose initial conditions for f so that it equals the largest root of the rhs of Eq. (15) at $\mu = 0$. The second face of Janus arises from analytically continuing the solution to negative values of μ. This can be implemented by brute force in numerics by taking the square root of Eq. (15) and multiplying the rhs by $\mathrm{sign}(\mu)$.

The main qualitative feature that distinguishes the Janus metric from undeformed AdS is that the boundary occurs at a value of the warped coordinate μ greater than $\pi/2$, the so-called angular excess [5–7]. The asymptotic behavior of the warp factor near the boundary is $f(\mu) \approx \frac{1}{\sin^2(\mu-\mu_0)}(1 + O(\mu-\mu_0)^8)$ [6], identical at leading order to the behavior AdS. The nonperturbative stability of this solution was shown in Ref. [6]. The dual gauge theory was studied in Ref. [7]. Many subsequent papers explored restoring supersymmetry in a Janus framework [8–14], adding a black hole [15,16], nesting Janus spacetimes of different dimension [17], and many other variations [18–32].

III. ADDING PROBE D7-BRANES WITH JANUS SLICING

Flavor is traditionally added to AdS/CFT via the prescription of adding N_f probe D7-branes that are spacetime filling in the AdS dimensions, wrapping a 3-cycle on the S5, and slipping off the pole of the S5 at some finite value of the warped coordinate, thus "ending in thin air" at that location [4]. In the dual theory, this corresponds to adding a number N_f of massive $\mathcal{N} = 2$ hypermultiplets in the fundamental representation of the gauge group. The probe limit means that the number of colors, N_c, is much greater than N_f, so any gravitational backreaction of the D7-branes on the metric can be neglected. As noted in Ref. [33], coordinate systems other than the Poincaré patch (or braneworld) do not readily admit an interpretation as the near horizon limit of a black D3-brane (or stack of N_c coincident such branes). So we follow the example of Ref. [33] and employ the strongest form of the AdS/CFT correspondence. Even if the dual gauge theory cannot be interpreted as the world volume theory of a stack of coincident D3-branes, $AdS_5 \times S^5$ with D7 flavor branes in a coordinate system other than the Poincaré patch is a perfectly valid supergravity system and should have a dual gauge theory description, regardless of the coordinate system or ansatz for the brane. In Ref. [33] flavor branes of various dimension were considered in global coordinates with the ansatz that the branes could fluctuate only in the radial, or ρ, direction. We will do the same in Janus-sliced coordinates, with the ansatz that the branes can only fluctuate in the μ direction. Much heuristic intuition can be gained by considering results from flavor branes in Poincaré patch coordinates and replacing $z \to \cos\mu$, effectively fixing the y coordinate to unity. This can serve as a guidepost for certain features, but many details are quite different in the Janus-sliced ansatz. We proceed under the assumption that our description of the dual gauge theory above is correct, exactly parallelling the original D3–D7 system except the natural spacetime for constructing this dual gauge theory consists of two copies of AdS_4 with their boundaries identified. By identifying boundaries, we mean that the boundary conditions for fields in one AdS_4 are related to the boundary conditions in the other, similar to the construction of Ref. [34].

We apply the same procedure in Janus-sliced coordinates both with and without the flowing dilaton of Janus itself. The D7-brane extends in the AdS directions and wraps an $S^3 \subset S^5$. The D7 is only allowed to fluctuate in the μ direction in Janus-sliced coordinates, and it extends from the boundary to some nonzero value of μ. When the flowing dilaton of Janus is added, we can no longer neglect the factor of the dilaton in the DBI action, and the equation of motion picks up additional terms from the dilaton. Recall that ϕ denotes the dilaton field, not an angle. We use Poincaré patch coordinates on the AdS_4 slices with y as the warped coordinate of the AdS_4 slices and take ψ and θ to be the two angles on the S5 that are transverse to the D7-brane. In regular AdS, the dirac-born-infeld (DBI) action for the Janus-sliced D7-brane has the same form as the usual case, but the warp factor is slightly different:

$$S \sim \int d^8x \cos^3(\psi(\mu))\frac{1}{\cos^3(\mu)}\sqrt{1+\cos^2(\mu)(\psi'(\mu))^2}. \tag{17}$$

The DBI action for full Janus can be obtained from Eq. (17) by substituting $\cos\mu \to f^{-1/2}(\mu)$ and inserting the factor $e^{-\phi(\mu)}$.

The resulting equation of motion is identical to the general equation of motion for D7-branes presented in Ref. [35], but we expand it here to highlight unique features in Janus-sliced coordinates:

$$0 = 3\,\tan\psi(\mu) + \frac{3\cos(\mu)\sin(\mu)\psi'(\mu) + 4\cos^3(\mu)\sin(\mu)\psi'(\mu)^3 + \cos^2(\mu)\psi''(\mu)}{1+\cos^2(\mu)\psi'(\mu)^2}. \tag{18}$$

Note that arcsine functions do not solve this equation of motion, unlike the original flavor brane ansatz, as can be easily checked by plugging in trial functions. We will turn to numerics to solve this equation of motion in Sec. III B.

A. Asymptotic expansion in Janus slicing

To examine the near boundary behavior of ψ, we expand our equations of motion about μ_0. As in Ref. [35], we will begin with the most general possible form for a power series expansion of $\psi(\mu)$. We will then substitute this into our equation of motion (EOM), expanded in terms of $v = \mu - \mu_0$, and examine the restrictions the EOM place on the coefficients of the expansion. According to the standard AdS/CFT dictionary, in order for the field ψ to properly describe a quark hypermultiplet mass operator in the boundary theory, its near boundary behavior should follow,

$$\psi(\mu) \approx A(\mu-\mu_0)^{\Delta} + B(\mu-\mu_0)^{d-\Delta}, \tag{19}$$

with $\Delta = 3$. Thus, the leading behavior should be

$$\psi(v) = Av + Bv^3. \tag{20}$$

The general expansion for $\psi(v)$ has the form [35]

$$\psi(\mu) = v\Bigg\{\sum_{n=0}^{\infty}\alpha_n v^n + \sum_{j=0}^{\infty}\beta_j v^j\,\log(v) + \sum_{k=0}^{\infty}\sum_{l=2}^{p}\Psi_{k,l}v^k[\log(v)]^l\Bigg\}. \tag{21}$$

We note that this expansion hinges on writing the metric in Fefferman–Graham coordinates [35], and in principle the coefficients of both the expansion of the metric in Fefferman–Graham coordinates and the expansion of bulk fields can be functions of other coordinates than the warped coordinate. The full implementation of Fefferman–Graham coordinates in Janus-sliced coordinates was carried out in Ref. [36]; however, for our brane ansatz, the bulk fields cannot vary with any coordinate other than μ, so we may safely ignore dependence of the coefficients on AdS_4 coordinates. The Janus warp factor, $f(\mu)$, has the same near boundary behavior as the $1/\cos^2(\mu)$ of ordinary AdS_5, and may be treated as [5,6]

$$f(v) \approx \frac{1}{\sin^2(v)} \approx \frac{1}{(v-\frac{1}{6}v^3)^2} \tag{22}$$

in the EOM. Furthermore, the dilaton field contributes to the EOM, only through its first μ derivative. Thus, we can see from Eq. (14) that it may be expanded as

$$\phi'(v) \approx c_0\sin^3(v) \approx c_0(v-\frac{1}{6}v^3)^3. \tag{23}$$

Below, we will keep the notation compact by denoting

$$X = \sin(v)$$
$$Y = -2\,\sin(v)\cos(v) \tag{24}$$

and later expanding these trigonometric functions in their appropriate power series.

Our equation of motion for ψ then takes on the near boundary form

$$X^2\psi'' + [1+X^2(\psi')^2]3\,\tan(\psi) + \frac{3}{2}Y\psi' + 2YX^2\psi' - [1+X^2(\psi')^2]X^5c_0\psi' = 0. \tag{25}$$

The explicit dilaton contribution is clearly identifiable, due to the factor of c_0, and can be seen to contribute only at order v^5 and higher. Since the leading asymptotic behavior of the warp factor is the same for both the Janus and ordinary AdS solutions, and the explicit dilaton terms in the Janus solution appear beyond the relevant order of v^3, we can conclude that this expansion will proceed identically for both cases. Thus, the asymptotic behavior found below, will apply to both the Janus solution and the "sliced branes" in ordinary AdS_5.

To confirm the proper asymptotic behavior for ψ, we must expand the EOM to order v^3. When we explicitly expand Eq. (25) in powers of v, including all terms relevant up to order v^3, we find

$$\left(v^2-\frac{1}{3}v^4\right)^2\psi'' + 3\left(\psi+\frac{1}{3}\psi^3\right) + 3v^2\psi(\psi')^2 - (3v+2v^3)\psi' = 0. \tag{26}$$

At first glance, it seems there may be many contributing terms. However, examining the EOM expansion (21) at lower orders in v, and looking at both the lowest and the highest powers of $\log(v)$, will reveal some simplifying restrictions:

$$0 = v\{(-\beta_0+2\Psi_{0,2}) + (6\Psi_{0,3}-4\Psi_{0,2})\log(v) + \cdots + (p-1)[p\Psi_{0,p}-2\Psi_{0,p-1}][\log(v)]^{p-2} - 2p\Psi_{0,p}[\log(v)]^{p-1}\}. \tag{27}$$

Recall, that l denotes an integer greater than 1. If we assume that $\Psi_{0,l}$ vanishes for $l = p$ and higher, then the second-to-last $\log(v)$ term tells us that $\Psi_{0,p-1}$ must also vanish, and so

on down the line. If there had been a contribution proportional to $\beta_0 v\,\log(v)$, this would have allowed a linear combination of β_0 and $\Psi_{0,2}$ to vanish as the coefficient of the $v\,\log(v)$ term. However, this is not the case, as the $\beta_0 v\,\log(v)$ terms from the portions of the EOM linear in ψ and ψ' cancel with one another. As noted in Ref. [35], an infinite tower of terms higher order in $\log(v)$ could exist, but this would invalidate the assumption of the existence of the power series solution. The same argument can also be shown to apply to the various $\Psi_{k,l}$ with $k \geq 1$. Thus, our power series solution for ψ actually has the simpler form

$$\psi(v) = v\left\{\sum_{n=0}^{\infty}\alpha_n v^n + \sum_{j=0}^{\infty}\beta_j v^j\,\log(v)\right\}. \tag{28}$$

This mirrors the form found in Ref. [35], with the radial coordinate r, which vanishes at the boundary, replaced by our $v = \mu - \mu_0$, which also vanishes at the boundary (μ_0 being equal to $\pi/2$ in the case of ordinary AdS_5.) Also note that notation for the expansion coefficients varies in the literature. For example, Ref. [35] uses $\phi_{(i)}$ where Ref. [33] used $\theta_{(i)}$. We chose $\alpha_{(i)}$ to minimize confusion between expansion coefficients and angles corresponding to supergravity fields.

Inserting this simpler expansion for ψ into the EOM, we can examine the leading order terms for further restrictions on the remaining coefficients. The first and second order pieces give

$$v\{-\beta_0\} = 0, \tag{29}$$

$$v^2\{-\alpha_1 - \beta_1\,\log(v)\} = 0. \tag{30}$$

From the lowest order term, it is clear that $\beta_0 = 0$. The second order contribution reveals that $\alpha_1 = \beta_1 = 0$. The vanishing of β_0 ensures that there will be no higher powers of $\log(v)$ contributed by the $(\psi)^3$ and $\psi(\psi')^2$ terms in the EOM. Thus, the order v^3 contribution will be

$$v^3\{\beta_2 - 6\alpha_0 + 6\alpha_0^3\} = 0. \tag{31}$$

The coefficient α_0 will thus be undetermined. The coefficients β_0, β_1, and α_1 will vanish. Then, α_0, when fixed, will determine the value of β_2 though the algebraic equation

$$\beta_2 = 6\alpha_0(1 - \alpha_0^2). \tag{32}$$

This same essential behavior (with a different algebraic equation relating β_2 and α_0) was found in Ref. [35]. Insuring that it applies here as well confirms that our branes—which are embedded differently due to the radial coordinate μ picked out by the Janus solution—will still properly describe fermion flavors in the boundary theory. This applies equally well in ordinary AdS_5 and Janus spaces.

B. Numerics

To solve Eq. (18) numerically, we denote by μ_b the ending location of the brane and use as initial conditions $\psi(\mu_b) = \pi/2 - \epsilon$, $\psi'(\mu_b) = -1/\epsilon$ with $\epsilon = 10^{-3}$ to approximate the usual conditions that the brane slip off the north pole with an infinite derivative. We present a few sample solutions to the equation of motion in Fig. 1; the numeric solution is shown in red (upper curve), and the function $\arcsin(\cos\mu/\cos\mu_b)$ is shown in blue for comparison. We plot solutions for three different values of μ_b on the same axes, for reference.

For large μ_b (and thus large mass), the Arcsine function is close to the actual solution, but it gets increasingly inaccurate as μ_b decreases. Per the asymptotic expansion, we fit the numeric solutions to $\alpha_{(0)}(\pi/2-\mu) + \alpha_{(2)}(\pi/2-\mu)^3$, where we have reversed the sign of the difference, v, introduced at the beginning of Sec. III A. The sign reversal is for convenience, so that we plot mostly positive masses, as an overall sign can be introduced in the dual gauge theory by a chiral rotation. For reference, we list the fit parameters for the example solutions shown in Fig. 1. For $\mu_b = 0.5$ we obtain $\alpha_{(0)} = 0.203805$, $\alpha_{(2)} = 1.21054$. For $\mu_b = 1.0$ we find fit parameters of 1.40824 and 3.31012, respectively. Finally for $\mu_b = 1.3$ we find 3.53835 and 12.2155.

To obtain plots for studying the phase structure of this system, we numerical solve and fit Eq. (18) successively from $\mu_b = 1.4$ down to $\mu_b = 0.1$ in steps of 0.01, then adjust the step size successively to 10^{-5}, 10^{-7}, and 10^{-12} for reasons that will become apparent. Recall that in Ref. [4] with arcsine solutions the mass was given by the inverse of the position where the brane ended. For Janus-sliced flavor branes, the relation between mass $(\alpha_{(0)})$ and μ_b is more complicated, given by Fig. 2. For values of μ_b near $\pi/2$, this has approximately the same shape as $1/\cos\mu_b$, as one might expect from naively extending the

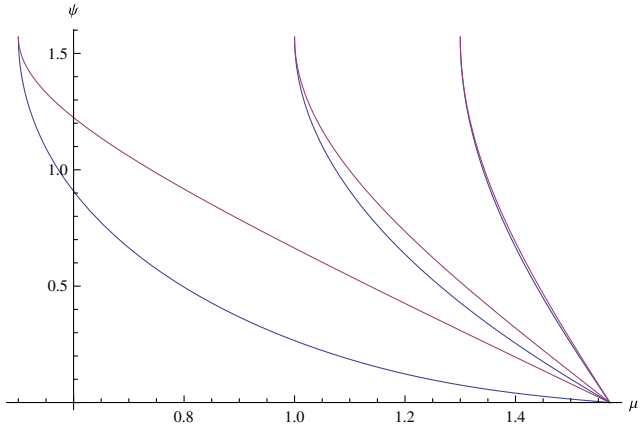

FIG. 1 (color online). ψ vs μ [in red (upper curve)] and $\arcsin(\mu/\mu_b)$ [in blue (lower curve)], for $\mu_b = 0.5$, 1.0, 1.3.

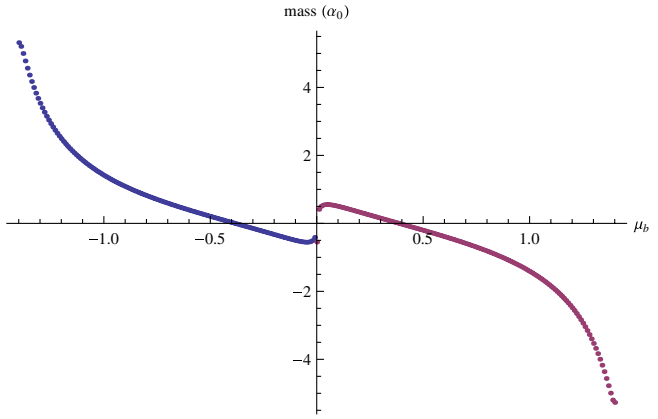

FIG. 2 (color online). Mass vs μ_b for disconnected flavor branes.

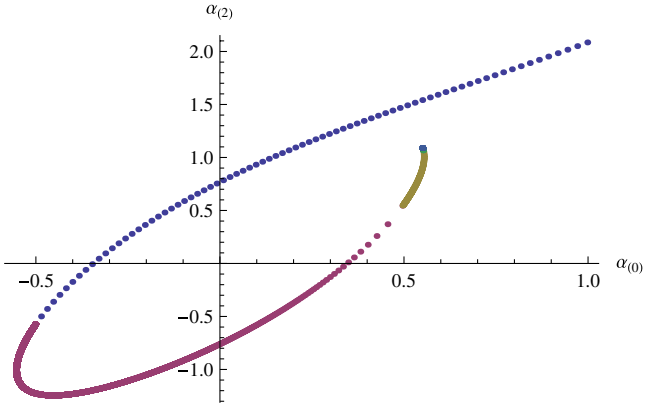

FIG. 4 (color online). $\alpha_{(2)}$ vs $\alpha_{(0)}$ for disconnected flavor branes detail.

relation from Ref. [4] with the Poincaré patch slicing using $z = y\cos\mu$, but the relationship is more subtle for lower mass configurations.

We plot $\alpha_{(2)}$ vs $\alpha_{(0)}$ in Fig. 3, zooming in to give detail in Fig. 4. The colors used denote the step size taken in μ_b. The blue curve ends at $\mu_b = 0.01$, the red curve at $\mu_b = 10^{-5}$, the yellow curve at $\mu_b = 10^{-7}$, and the green curve (which appears more as a dot) at $\mu_b = 10^{-12}$. The step size for each color is equal to the ending value of μ_b. At first, near $\mu_b = 0.01$ and again near $\mu_b = 10^{-5}$, it appears that we are making bigger and bigger steps in the $\alpha_{(2)} - \alpha_{(0)}$ plane as we approach $\mu_b = 0$. But then the curve appears to stop abruptly at $\mu_b = 10^{-12}$.

There appears to be a kind of limit point in the numerical solutions approaching $\alpha_{(0)} = 0.5501$, $\alpha_{(2)} = 1.08895$ as $\mu_b \to 0$. Note, however, that it is impossible to impose "brane ending" boundary conditions at $\mu_b = 0$. The boundary condition that $\psi(\mu) \to \pi/2$ causes the tan $\psi(\mu)$ term to diverge. For nonzero μ_b the accompanying boundary condition that $\psi'(\mu) \to \infty$ naturally cancels this divergence when both are implemented as $\psi(\mu_b) = \pi/2 - \epsilon$, $\psi'(\mu_b) = 1/\epsilon$.

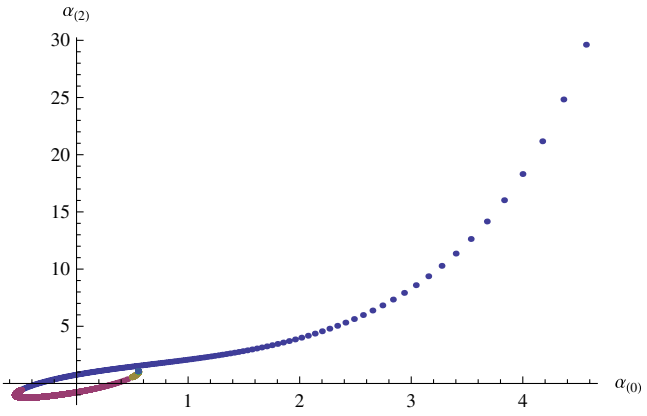

FIG. 3 (color online). $\alpha_{(2)}$ vs $\alpha_{(0)}$ for disconnected flavor branes.

Unfortunately, when $\mu_b = 0$ the coefficients of all the ψ' terms in the equation of motion vanish, reducing the equation of motion to $0 = 3\tan\psi(\mu) + \psi''(\mu)/(1+\psi'(\mu)^2)$. Imposing both boundary conditions simultaneously requires infinite $\psi''(0)$ and cannot be solved numerically. If we try a series expansion near $\mu = 0$, similar to the expansion in Ref. [33], promoting the infinitesimal ε to a small fluctuation, $\psi = \pi/2 - \varepsilon(\mu)$, the action reduces to

$$S \sim \int d^8x\left(-\varepsilon(\mu)^3\sqrt{1+(\psi'(\mu))^2}\right). \tag{33}$$

The resulting equation of motion is

$$\varepsilon^2(\mu)(-3-3(\varepsilon'(\mu))^2+\varepsilon(\mu)\varepsilon''(\mu)) = 0, \tag{34}$$

which does not have an analytic solution except for the trivial one, $\varepsilon = 0$. The action and lack of a nontrivial solution are consistent with the series expansions in Ref. [33] for branes of general dimension that extend in j of the AdS dimensions and i of the S^5 dimensions. Our action for $\mu \sim 0$ in Janus-sliced coordinates is similar to the action of Ref. [33] for $i = 2$, and the critical solution, Eq. (3.4) of Ref. [33], does not exist for the $i = 2$ case. This analysis does not rule out the possibility of other solutions not detected by our numerics that would continue the spiral of Fig. 4 down to $\alpha_{(0)} = 0$, $\alpha_{(2)} = 0$; however, if a nontrivial such solution exists, it does not reach the origin of Fig. 4 at $\mu_b = 0$. This would be extremely puzzling, since this is ordinary AdS space where there is nothing to set a scale or otherwise mark any location other than $\mu_b = 0$ as special.

We find evidence of spontaneous chiral symmetry breaking in Fig. 4. The mass ($\alpha_{(0)}$) reaches zero between $\mu_b = 0.38$ and 0.39. Since this occurs with $\alpha_{(2)}$ between 0.75398 and 0.784872, we conclude that the dual theory will exhibit spontaneous chiral symmetry breaking as the mass of the quarks is taken zero. Note that Fig. 4 describes a brane confined to one-half of the boundary, at either

$\mu = +\pi/2$ or $\mu = -\pi/2$. Chiral symmetry breaking is assured as long as the number of disconnected branes on either side is unequal. The possibility exists that an equal number of disconnected branes on either side might not truly break chiral symmetry as this state may possess higher free energy than the trivial, supersymmetric D7 with constant equatorial (on the S^5) embedding. However, we believe the disconnected brane embedding to be at least metastable. Dynamically evolving from the disconnected state to the trivial embedding would require the disconnected D7s to "unslip" (i.e., for the collapsed S^3 to reappear and slide down from the pole of the S^5) before they could merge, as Eq. (18) does not admit a solution for the collapsed S^3 boundary condition occurring at $\mu_b = 0$ as discussed above. It may prove to be the case that disconnected Janus-sliced embeddings should not be compared to the trivial embedding due to these dynamical concerns. We will explore these questions, including questions of free energy, in detail in future work.

Chiral symmetry breaking would be expected for Janus proper, but it is surprising to find it in undeformed AdS simply with Janus-sliced flavor branes. Interestingly, this chiral symmetry breaking is not detected by the test proposed in Refs. [37,38], but the geometry in our case is sufficiently different from the backgrounds considered there that this is not too surprising. In particular, there is no central singularity in our geometry, so the criteria used in Ref. [37] do not apply.

C. Asymmetric and continuous flavor branes

Janus-sliced coordinates do not exhibit a horizon, so the possibility exists for a D7-brane to extend across the full range of μ, from the "right-hand" boundary at $\mu = \pi/2$, through the "center" at $\mu = 0$, and out to the "left-hand" boundary at $\mu = -\pi/2$. Indeed, the trivial solution, $\psi(\mu) = 0$, obviously exists and gives zero mass and zero vacuum expectation value quarks in the dual theory[1]. Furthermore, the flavor branes examined in Sec. III B fill only half the spacetime, so quarks in the dual theory would exist in only one of the two AdS_4 spaces. Since the geometry is symmetric under $\mu \to -\mu$, it is trivial to extend these results by adding a mirror image brane extending from $\mu = -\pi/2$ to $-\mu_b$. This is borne out by numerics: numerically solving Eq. (18) from $\mu = -\pi/2$ to $\mu_b < 0$ yields results for $\alpha_{(0)}$ and $\alpha_{(2)}$ that differ from the values for the corresponding positive μ_b by at most $O(10^{-3})$. For a given μ_b, this would give quarks in the dual theory with mass constant across both AdS_4 spaces. However, the two branes are disconnected in the bulk, so there is nothing beyond aesthetics imposing symmetry. The D7-brane in the negative μ half of space may end at a different distance than the D7 in the positive μ half of space. The dual theory in such a case would have quark masses that were constant on each AdS_4 but different between the two AdS_4 spaces.

Continuous branes can also exhibit this asymmetry. Generic solutions to Eq. (18) for continuous branes exhibit different asymptotic behavior at the two boundaries. If initial conditions are chosen for a continuous brane solution such that the center of AdS, $\mu = 0$, is a turning point for ψ, then the symmetry of the geometry guarantees that the behavior of ψ will be symmetric at the two boundaries as well. This, too, is borne out by numerics to $O(10^{-3})$. For continuous brane solutions, we solve Eq. (18) numerically imposing boundary conditions at $\mu = 0$. For the symmetric mass cases, we impose $\psi'(0) = 0$, $\psi(0) = c$, where c is a real parameter we step through from -1.57 to +1.57. For a sample solution in this class, see Fig. 5. For generic cases, we allow the first derivative to be nonzero, giving a two-parameter family of solutions. See Fig. 6 for a sample solution in this class.

The easiest to understand data on continuous brane solutions come from the symmetric case. We plot $\alpha_{(2)}$ vs $\alpha_{(0)}$ for symmetric continuous branes as $\psi(0)$ ranges from -1.57 to +1.57 in steps of 0.005 in Fig. 7. The plot begins at the origin for $\psi(0) = 0$, corresponding to the trivial solution. The two spiral arms are symmetric and stem from the fact that changing the sign of $\psi(0)$ in this case simply changes the sign of both fit parameters in the asymptotic solution. The blue curve represents solutions with $\psi(0) < 0$. The red curve represents $\psi(0) > 0$ and extends out to $\psi(0) = 1.5707$, with the step size reducing to $\Delta\psi(0) = 10^{-4}$ after we reach $\psi(0) = 1.57$, then reducing again to $\Delta\psi(0) = 10^{-6}$ when we reach $\psi(0) = 1.5707$. The fact that the red curve overlaps the blue so completely is surprising. It certainly indicates that continuous branes cannot produce quarks with arbitrarily large mass. The maximum value of mass in our runs is $m = 0.551489$. The near perfect overlap of the two curves suggests that a phase transition may occur between different types of symmetric, continuous branes: one with positive value of $\psi(0)$ very close to $\pi/2$ and one with a more modest, negative value of

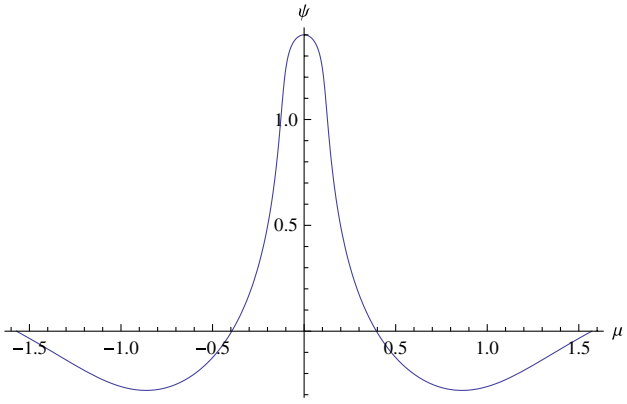

FIG. 5 (color online). ψ vs μ for a continuous brane solution with $\psi(0) = +1.4$, $\psi'(0) = 0$.

[1]We are indebted to A. Karch for these observations.

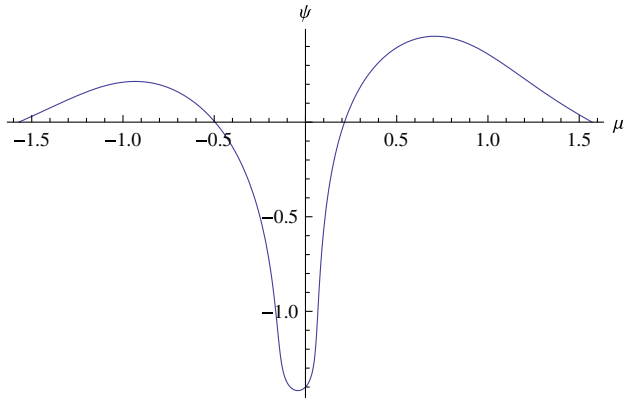

FIG. 6 (color online). ψ vs μ for a continuous brane solution with $\psi(0) = -1.4$, $\psi'(0) = +1$.

$\psi(0)$ (and vice versa). The doubling back of the curves also indicates that spontaneous chiral symmetry breaking occurs for continuous flavor branes with $\psi(0) \lesssim 1.57$, where it appears the curve crosses the $\alpha_{(2)}$ axis with nonzero intercept, indicating a nonzero vacuum expectation value at zero mass. Note that while this seems a value extremely close to $\pi/2$, it occurs well before the region of the possible phase transition. Note that Fig. 7 includes the trivial solution (flat, equatorial D7 preserving chiral symmetry) at the origin. As in the disconnected case, future work will compare the free energy of the chiral breaking embedding compared to the trivial embedding and explore questions of the stability of the chiral breaking embedding.

More generic continuous brane solutions require us to fit the asymptotic solution at $\mu = +\pi/2$ and $\mu = -\pi/2$ separately. We use subscripts "R" and "L," respectively, to denote these different sets of fit parameters. We present our results as a pair of contour plots, Figs. 8 and 9, treating $\alpha_{(2)L}$ and $\alpha_{(2)R}$ as dependent variables that depend on the pair of independent variables $(\alpha_{(0)L}, \alpha_{(0)R})$. Note the apparent mirror image relationship between the two contour plots.

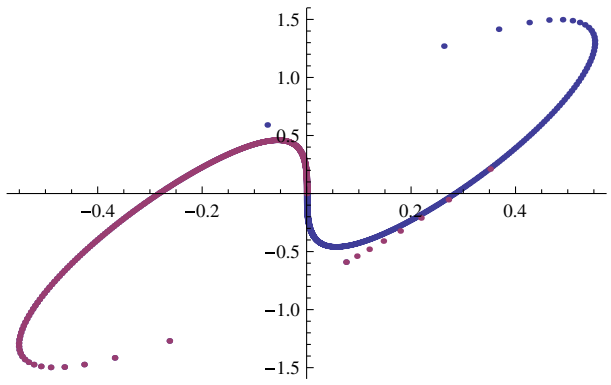

FIG. 7 (color online). $\alpha_{(2)}$ vs $\alpha_{(0)}$ for symmetric, continuous branes.

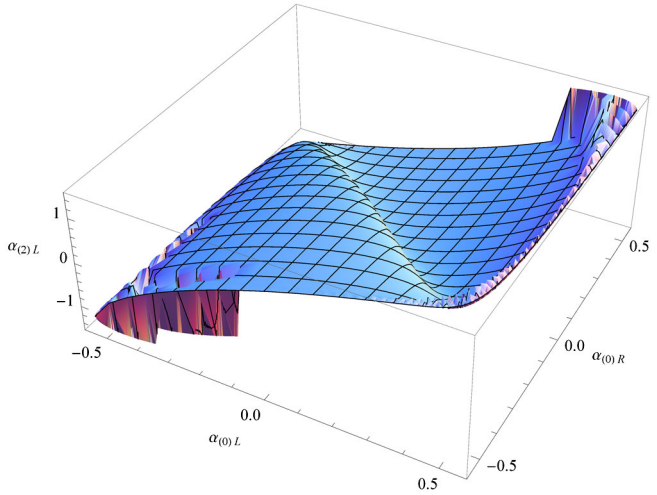

FIG. 8 (color online). $\alpha_{(2)L}$ vs $\alpha_{(0)L}$ and $\alpha_{(0)R}$ for general continuous branes.

IV. APPARENT LACK OF PHASE TRANSITION BETWEEN DISCONNECTED AND CONTINUOUS FLAVOR BRANES

The natural expectation is that for low mass continuous branes might be favored, while for larger mass disconnected branes might be favored. This does not prove to be the case, however. In Fig. 10 we overlay the plots from Figs. 4 and 7 but use blue and red to denote the symmetric brane configurations. While the curves cross at various points, we do not see the telltale merging of the plots that would signal a phase transition. We tried looking for other classes of solutions to fill in the phase diagram; in particular we considered disconnected branes that crossed the center of AdS at $\mu = 0$ and "bubble" branes that pinched off at both a positive and a negative value of μ and extended through the center. Both seemed to be ruled out by numerics. Attempting to impose boundary conditions

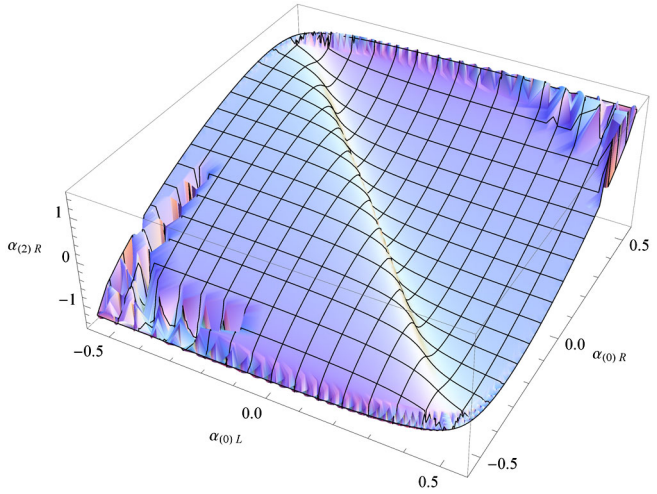

FIG. 9 (color online). $\alpha_{(2)R}$ vs $\alpha_{(0)L}$ and $\alpha_{(0)R}$ for general continuous branes.

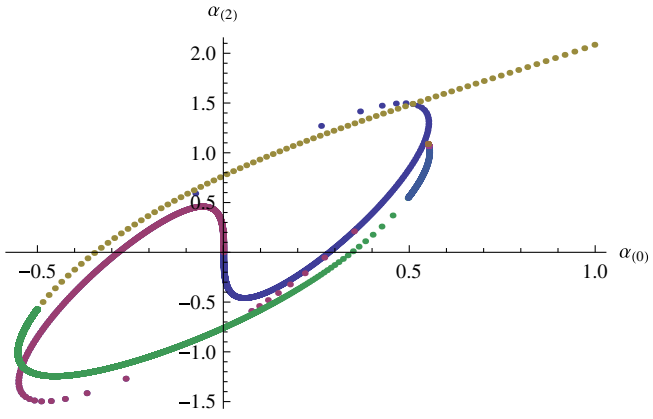

FIG. 10 (color online). $\alpha_{(2)}$ vs $\alpha_{(0)}$ overlay plot for both symmetric-continuous and disconnected branes.

$\psi(\mu_b) \approx \pi/2$, $\psi'(\mu_b) \approx \infty$ (necessary for both classes) while solving for $0 < \mu < \mu_b$ immediately encounters a singularity to the left of μ_b when a numeric solution is attempted.

While it remains possible that there exists some class of solutions which we have not discovered, we speculate that the lack of phase transition is because disconnected flavor branes and continuous flavor branes describe incommensurate dual gauge theories. For example, with disconnected branes, even if the masses are chosen to be equal, one need not even choose to use the same number of branes on the left and right sides of AdS. The fact that this option is simply unavailable in the case of continuous branes is the first piece of evidence to suggest the two types of solutions are described by qualitatively different dual gauge theories. A second piece of evidence is the lack of disconnected brane solutions pinching off at $\mu = 0$. Heuristically, we would have liked to think of the (nonexistent) phase transition as occurring when flavor branes on the left and right sides of AdS approached the center and merged. However, in Sec. III B we showed that disconnected branes simply cannot "pinch off" at $\mu = 0$. This was shown both at the large scale from the failure of Eq. (18) to accommodate the "brane pinching off" boundary conditions at $\mu = 0$ and at the small scale (small values of μ) by the failure of Eq. (34) to admit nontrivial solutions in the vicinity of $\mu = 0$. If disconnected branes can never reach or cross $\mu = 0$, then there is no hope of achieving a phase transition by melding disconnected branes from the left and right halves of AdS in Janus-sliced coordinates.

Since the disconnected branes are confined to one-half of the bulk AdS_5, we speculate that the dual gauge theories for disconnected and continuous brane solutions differ in the boundary conditions for the quark hypermultiplet fields at the boundary between the two AdS_4 halves of the boundary theory. A disconnected brane on the right side of AdS_5 seems to naturally correspond to a quark hypermultiplet restricted to the "right" AdS_4 in the dual gauge theory with "perfectly reflecting" boundary conditions at the boundary between the two AdS_4 half-spaces. A continuous flavor brane, however, should correspond to quarks that can freely traverse from the right AdS_4 to the "left," corresponding to "transparent" boundary conditions where the leading and subleading terms on the two boundary AdS_4 spaces match. The phrases perfectly reflecting and transparent boundary conditions are meant only in a heuristic sense, as we are discussing solutions to the equations of motion for fields of arbitrary mass in AdS_4, which must have the well-known asymptotic form $\phi_\Delta \sim a y^\Delta + b y^{d-\Delta}$, where y denotes the warped coordinate in the Poincaré slicing of the boundary AdS_4 ($d = 3$ in the general formula). The mass from the AdS_4 equation of motion and the dimension Δ are related by Witten's venerable prescription [2], and both are determined by the solutions of the D7 slipping mode in the bulk. Denoting the two boundary AdS_4 spaces as L and R, we can phrase our boundary conditions more precisely: perfectly reflecting means a field in AdS_{4L} does not provide a corresponding source in AdS_{4R} (and vice versa), thus requiring $a_L = 0$ for a quark field in AdS_{4L} (and similarly for a_R and quarks in AdS_{4R}); transparent means $a_L = a_R$ and $b_L = b_R$, allowing the field to propagate unaltered from AdS_{4L} to AdS_{4R} in a heuristic sense.

If this is the correct interpretation of the dual gauge theory, then there clearly cannot be a phase transition as the two scenarios are completely different. However, this hypothesis poses additional puzzles. If continuous flavor branes indeed describe an $\mathcal{N} = 2$ hypermultiplet with transparent boundary conditions between the two AdS_4 spaces, there should be no obstacle to large quark mass solutions. Yet the continuous brane solutions do not seem to admit solutions with quark mass larger than about $m_{L,R} = 0.551$. While it is difficult to see this in the contour plots of Figs. 8 and 9, it remains true for generic, asymmetric continuous branes as well. The most likely answer is that a second class of continuous flavor brane solutions exists that was not detected by our numerics and admits large mass solutions, although the space of possible alternative explanations is by definition infinite.

V. FLAVOR BRANES IN JANUS

The dynamical factor of the DBI action for such a D7-brane in Janus is

$$S \sim \int d^8x e^{-\phi(\mu)} \cos^3\psi(\mu) f^2(\mu) \sqrt{f(\mu) + (\psi'(\mu))^2}. \quad (35)$$

This gives rise to the following equation of motion for ψ:

$$\begin{aligned} 0 = {} & \frac{f(\mu)\cos^2\psi(\mu)}{2(f(\mu) + (\psi'(\mu))^2)^{3/2}} (6 \sin\psi(\mu) f(\mu)^2 (f(\mu) + \psi'(\mu)^2) \\ & + \cos(\psi(\mu))(4\psi'(\mu)^3 f'(\mu) + f(\mu)(3\psi'(\mu) f'(\mu) \\ & - 2\psi'(\mu)^3 \varphi'(\mu)) + 2f(\mu)^2(-\psi'(\mu)\varphi'(\mu) + \psi''(\mu)))). \end{aligned} \quad (36)$$

Qualitatively, turning on the dilaton of Janus does exactly as little as we expect it to thus far: the warp factor is changed slightly, the boundary is pushed out beyond $\mu = \pi/2$, and the equation of motion for our Janus-sliced flavor branes picks up some extra terms proportional to the derivative of the dilaton field.

Numerically solving Eq. (36) with the same brane pinching off boundary conditions as in regular AdS for $c_0 = 0.2$, 0.8, and 1.2, we obtain Fig. 11. The left end of each curve corresponds to $\mu_b = 0.2$. Note that the same qualitative shape found for Janus-sliced flavor branes in undeformed AdS is present. As c_0 increases, the shape of the curve changes more and more and more radically, changing convexity and flipping over to the fourth quadrant for $c_0 = 1.2$.

VI. IMPLICATIONS IN DUAL THEORY

Roughly speaking, the natural choice of the conformal factor in AdS slicing gives a dual theory on two copies of AdS_4 joined at their common boundary. If we make this choice for Janus-sliced flavor branes in undeformed AdS, we would expect to find that the quark mass jumps as one crossed the boundary from one AdS_4 to the other. After studying Janus-sliced flavor branes in detail, we realize that far more dramatic changes could take place, such as changing the number of flavors. Different choices of the conformal factor and thus different coordinate systems in the dual gauge are of course allowed.

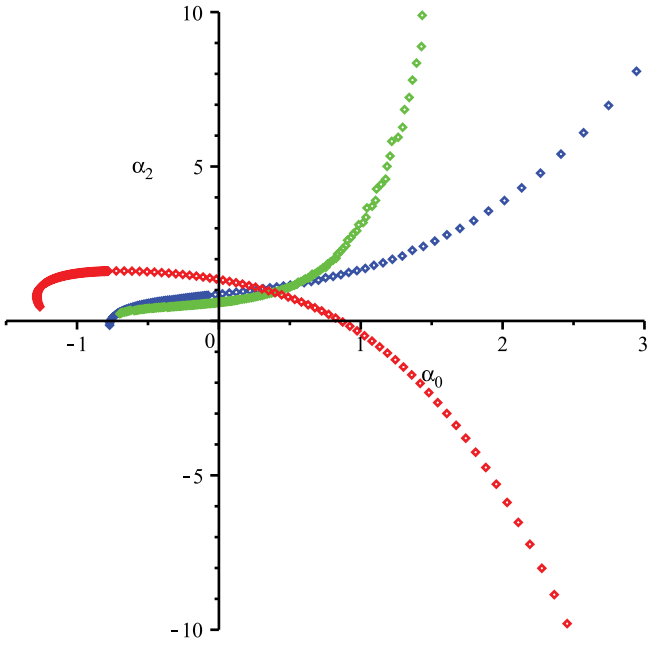

FIG. 11 (color online). $\alpha_{(2)}$ vs $\alpha_{(0)}$ for Janus. Green (steepest positive slope in first quadrant): $c_0 = 0.2$, blue (shallower positive slope in first quadrant): $c_0 = 0.8$, red (negative slope in fourth quadrant): $c_0 = 1.2$.

Following the general prescription of Ref. [2] for constructing the dual gauge theory and the refinements of Refs. [39,40], we obtain the boundary metric by multiplying the AdS metric by g^2, where g is any function with a linear zero at the boundary, often dubbed the "conformal factor." We are specializing to the case of Janus-sliced coordinates in the bulk. For a general bulk scalar field, ϕ_Δ, of dimension Δ, where x generically denotes the "nonwarped" directions of AdS_{d+1}, the near boundary behavior is given by

$$\varphi_\Delta \sim a_g(x)(g^{d-\Delta} + \cdots) + b_g(x)(g^\Delta + \cdots). \tag{37}$$

It is well known that a_g is the source of the dual operator and b_g is the vacuum expectation value, although the vacuum expectation value is in general a more complicated function of the leading and subleading coefficients using the prescription of holographic renormalization [35]. In the dual theory, changing metrics is accomplished with a conformal transformation. In the bulk theory, the same is realized by choosing a different conformal factor to regulate the boundary metric. To see the relationships between coefficients with different choices of the conformal factor, recall in the bulk the field is a scalar, so each term in the asymptotic expansion must be invariant. If we compare two conformal factors, g_1 and g_2, this gives us the relationship between two boundary coefficients of

$$a_{g1} = \left(\frac{g_2}{g_1}\right)^{d-\Delta} a_{g2}, \tag{38}$$

$$b_{g1} = \left(\frac{g_2}{g_1}\right)^{\Delta} b_{g2}. \tag{39}$$

A similar discussion centered on the operator dual to the dilaton field appears in Ref. [7]. Applying this to Janus-sliced flavor branes shows us that if we choose the conformal factor such that the dual theory lives on two copies of AdS_4, then the mass of the quarks will be piecewise constant. If we conformally transform to Minkowski space, examining metric (9), we see that the mass becomes a function of y in the dual theory,

$$m_{M_4} = \frac{m_{AdS_4}}{y}, \tag{40}$$

since the scalar field describing our D7-brane is of dimension 3. Massive quarks in actual Janus will be further complicated by the presence of the operator dual to the dilaton [7], but at leading order, this will not effect the position dependence of the mass operator in the dual theory. We postpone more detailed study of the dual theory for future work.

Since the phase diagrams of disconnected brane solutions and continuous brane solutions do not exhibit

behavior characteristic of a phase transition, we hypothesize that the two types of brane solutions are dual to qualitatively different gauge theories. We propose that continuous brane solutions are dual to an $\mathcal{N}=2$ hypermultiplet mass operator that has transparent boundary conditions at the shared boundary in AdS_4, in the sense discussed above ($a_L = a_R$ and $b_L = b_R$). Recall this is a statement about the AdS_4 boundary conditions necessary for solving the equations of motion of the fields of the $\mathcal{N}=2$ hypermultiplet in the dual field theory. That is to say, the leading and subleading terms of a solution to the equation of motion for a quark in the dual theory must be the same on both sides of the defect in the CFT, as discussed in more detail above.

Our proposal for the system dual to disconnected flavor branes is that this dual mass operator is for quark fields that exhibit "totally reflecting" boundary conditions in the sense discussed above and are confined to one of the boundary AdS_4 spaces. Disconnected flavor branes extending to the right boundary do not have any impact on fields in the left boundary and vice versa. We think this is the most likely case for several reasons. First, from the gravity side, we could choose to use a different number of flavor branes on each side of AdS_5, giving a different number of flavors in the two half-spaces in the dual theory. Second, since the value of the dual operator is determined by the leading order behavior of the gravity state in the bulk as it approaches the boundary, the coupling of the mass operator from a flavor brane in the right half of AdS_5 is literally undefined in the AdS_4 of the dual theory that corresponds to the left half of the bulk. A brane on the right ($\mu > 0$) does not exist on the left ($\mu < 0$), so the asymptotic behavior of that state as it approaches $\mu = -\pi/2$ is undefined. In the bulk, causality demands that, quite literally, the left brane does not know what the right brane is doing. We see no way to implement this in the dual theory without totally reflecting boundary conditions for the dual quarks in each half-space AdS_4.

We must impose totally transparent boundary conditions on gluons in the dual theory for both flavor brane scenarios, as those states are only sensitive to the existence or type of flavor branes through interactions with the quark states.

VII. CONCLUSION

We have proposed and analyzed Janus-sliced flavor branes as the appropriate system for studying the addition of flavor to the Janus solution. Janus-sliced coordinates on AdS_5 produce a theory most naturally dual to $\mathcal{N}=4$ super-Yang–Mills on two copies of AdS_4 joined at a common boundary. The main motivation for studying such a system is to look at Janus itself, but our numeric studies have uncovered a rich and surprising structure even in undeformed AdS_5 without turning on the flowing dilaton of Janus. Janus-sliced coordinates admit possibilities that do not exist in other coordinate systems: continuous flavor branes that extend from one boundary through the center of AdS out to the other boundary have been studied in global coordinates [33] but are not possible in the Poincaré patch, and asymmetric flavor branes that end at different positions on the two "halves" of AdS do not seem to be possible in any other coordinate system.

We have demonstrated that both disconnected and continuous branes exhibit spontaneous chiral symmetry breaking, each possessing a state with nonzero vacuum expectation value at zero mass. Disconnected flavor branes can produce states of arbitrarily large mass, while continuous branes (whether symmetric or not) yield solutions with mass bounded by approximately $m_{\max} = 0.551$ in units of the inverse AdS radius. This is one of many puzzles associated with the continuous flavor brane solutions, as there seems to be no compelling reason to restrict the mass of quarks in the dual gauge theory, suggesting the existence of yet another class of flavor brane solutions. There may also be a phase transition between continuous flavor branes with values of $\psi(0)$ near $+\pi/2$ and those near $-\pi/2$, indicated by the overlap in the phase diagram of Fig. 7. Analysis of the free energies of the brane configurations will be necessary to confirm the existence of such a phase transition.

Since there does not appear to be a phase transition between disconnected flavor branes and connected, we propose that disconnected flavor branes are dual to quark hypermultiplets with piecewise constant mass on AdS_4 with totally reflecting boundary conditions at the boundary of each AdS_4 half-space, whereas continuous flavor branes are dual to quark hypermultiplets with piecewise constant mass and totally transparent boundary conditions. In both cases, the entire gluon multiplet must have totally transparent boundary conditions. This proposal for differing quark boundary conditions on AdS_4 is further supported by gravity-side arguments such as causal disconnection of left and right branes as well as the fact that the number of flavor branes could be chosen to be different on each side.

We have also presented a phase diagram for quarks in Janus proper, using disconnected branes with $\mu_b > 0$ and three different values of the Janus parameter, c_0. The additional terms in the equation of motion arising from the flowing dilaton make the numerics intrinsically less stable in Janus proper than in undeformed AdS with Janus-sliced coordinates, so we cannot offer as much detail. Qualitatively, we see expected behavior, with large mass when μ_b is near μ_0 and solutions very similar to undeformed AdS when c_0 is small. Large c_0 begins to change qualitative features of the phase diagram, pushing the "turnaround point" for the spiral further to the left and reversing the convexity of the curve when c_0 is large enough. It will be important for future work to address the mysteries surrounding the continuous flavor brane solutions, determine whether a phase transition exists for "near polar" continuous flavor branes, and study the dual

theories we propose in Sec. VI. Future work will also explore questions of the free energy of Janus-sliced D7 embeddings in comparison to the trivial embedding to ascertain whether the symmetric cases studied here truly break chiral symmetry. It is very surprising that simply changing the flavor brane ansatz in this manner results in such a radical change of behavior. It will also be very interesting to study the exact mechanism by which chiral symmetry breaking occurs, both in the dual gauge theory and in the supergravity.

ACKNOWLEDGMENTS

A. B. C. and N. C. would like to thank J. Shock and B. Fadem for helpful conversations. A. B. C. would like to especially thank A. Karch for many patient and detailed conversations about the peculiarities of flavor branes with the Janus-sliced ansatz. The work of N. C. was partially supported by the Raub Fund. The work of A. B. C. was partially supported by a Faculty Summer Research Grant from the Office of the Provost of Muhlenberg College.

[1] J. M. Maldacena, Adv. Theor. Math. Phys. **2**, 231 (1998).
[2] E. Witten, Adv. Theor. Math. Phys. **2**, 253 (1998).
[3] S. Gubser, I. R. Klebanov, and A. M. Polyakov, Phys. Lett. B **428**, 105 (1998).
[4] A. Karch and E. Katz, J. High Energy Phys. 06 (**2002**) 043.
[5] D. Bak, M. Gutperle, and S. Hirano, J. High Energy Phys. 05 (**2003**) 072.
[6] D. Freedman, C. Nunez, M. Schnabl, and K. Skenderis, Phys. Rev. D **69**, 104027 (2004).
[7] A. Clark, D. Freedman, A. Karch, and M. Schnabl, Phys. Rev. D **71**, 066003 (2005).
[8] A. Clark and A. Karch, J. High Energy Phys. 10 (**2005**) 094.
[9] E. D'Hoker, J. Estes, and M. Gutperle, Nucl. Phys. **B757**, 79 (2006).
[10] E. D'Hoker, J. Estes, and M. Gutperle, Nucl. Phys. **B753**, 16 (2006).
[11] E. D'Hoker, J. Estes, and M. Gutperle, J. High Energy Phys. 06 (**2007**) 021.
[12] M.-W. Suh, J. High Energy Phys. 09 (**2011**) 064.
[13] C. Kim, E. Koh, and K.-M. Lee, Phys. Rev. D **79**, 126013 (2009).
[14] E. D'Hoker, J. Estes, and M. Gutperle, J. High Energy Phys. 06 (**2007**) 022.
[15] D. Bak, M. Gutperle, and S. Hirano, J. High Energy Phys. 02 (**2007**) 068.
[16] D. Bak, M. Gutperle, and R. A. Janik, J. High Energy Phys. 10 (**2011**) 056.
[17] S. Hirano, J. High Energy Phys. 05 (**2006**) 031.
[18] C. Bachas and J. Estes, J. High Energy Phys. 06 (**2011**) 005.
[19] T. Nishioka and H. Tanaka, J. High Energy Phys. 02 (**2011**) 023.
[20] M. Chiodaroli, M. Gutperle, and L.-Y. Hung, J. High Energy Phys. 09 (**2010**) 082.
[21] M. Chiodaroli, E. D'Hoker, and M. Gutperle, J. High Energy Phys. 03 (**2010**) 060.
[22] M. Chiodaroli, M. Gutperle, and D. Krym, J. High Energy Phys. 02 (**2010**) 066.
[23] E. D'Hoker, J. Estes, M. Gutperle, and D. Krym, J. High Energy Phys. 09 (**2009**) 067.
[24] E. D'Hoker, J. Estes, M. Gutperle, and D. Krym, J. High Energy Phys. 06 (**2009**) 018.
[25] S. Ryang, J. High Energy Phys. 05 (**2009**) 009.
[26] B. Chen, Z.-b. Xu, and C.-y. Liu, J. High Energy Phys. 02 (**2009**) 036.
[27] Y. Honma, S. Iso, Y. Sumitomo, and S. Zhang, Phys. Rev. D **78**, 025027 (2008).
[28] D. Gaiotto and E. Witten, J. High Energy Phys. 06 (**2010**) 097.
[29] C. Kim, E. Koh, and K.-M. Lee, J. High Energy Phys. 06 (**2008**) 040.
[30] T. Azeyanagi, A. Karch, T. Takayanagi, and E. G. Thompson, J. High Energy Phys. 03 (**2008**) 054.
[31] D. Bak, Phys. Rev. D **75**, 026003 (2007).
[32] J. Sonner and P. K. Townsend, Classical Quantum Gravity **23**, 441 (2006).
[33] A. Karch, A. O'Bannon, and L. G. Yaffe, J. High Energy Phys. 09 (**2009**) 042.
[34] O. Aharony, A. B. Clark, and A. Karch, Phys. Rev. D **74**, 086006 (2006).
[35] A. Karch, A. O'Bannon, and K. Skenderis, J. High Energy Phys. 04 (**2006**) 015.
[36] I. Papadimitriou and K. Skenderis, J. High Energy Phys. 10 (**2004**) 075.
[37] N. Evans, J. P. Shock, and T. Waterson, J. High Energy Phys. 03 (**2005**) 005.
[38] N. J. Evans and J. P. Shock, Phys. Rev. D **70**, 046002 (2004).
[39] V. Balasubramanian, P. Kraus, and A. E. Lawrence, Phys. Rev. D **59**, 046003 (1999).
[40] V. Balasubramanian, P. Kraus, A. E. Lawrence, and S. P. Trivedi, Phys. Rev. D **59**, 104021 (1999).